

Diffusion-weighted imaging of breast lesions: Region-of-interest placement and different ADC parameters influence apparent diffusion coefficient values

Hubert Bickel¹ · Katja Pinker¹ · Stephan Polanec¹ · Heinrich Magometschnigg¹ · Georg Wengert¹ · Claudio Spick¹ · Wolfgang Bogner² · Zsuzsanna Bago-Horvath³ · Thomas H. Helbich¹ · Pascal Baltzer¹

Received: 9 June 2016 / Accepted: 11 August 2016 / Published online: 30 August 2016
© European Society of Radiology 2016

Abstract

Objectives To investigate the influence of region-of-interest (ROI) placement and different apparent diffusion coefficient (ADC) parameters on ADC values, diagnostic performance, reproducibility and measurement time in breast tumours.

Methods In this IRB-approved, retrospective study, 149 histopathologically proven breast tumours (109 malignant, 40 benign) in 147 women (mean age 53.2) were investigated. Three radiologists independently measured minimum, mean and maximum ADC, each using three ROI placement approaches: 1 – small 2D-ROI, 2 – large 2D-ROI and 3 – 3D-ROI covering the whole lesion. One reader performed all measurements twice. Median ADC values, diagnostic performance, reproducibility, and measurement time were calculated and compared between all combinations of ROI placement approaches and ADC parameters.

Results Median ADC values differed significantly between the ROI placement approaches ($p < .001$). Minimum ADC showed the best diagnostic performance (AUC .928–.956),

followed by mean ADC obtained from 2D ROIs (.926–.94). Minimum and mean ADC showed high intra- (ICC .85–.94) and inter-reader reproducibility (ICC .74–.94). Median measurement time was significantly shorter for the 2D ROIs ($p < .001$).

Conclusions ROI placement significantly influences ADC values measured in breast tumours. Minimum and mean ADC acquired from 2D-ROIs are useful for the differentiation of benign and malignant breast lesions, and are highly reproducible, with rapid measurement.

Key Points

- Region of interest placement significantly influences apparent diffusion coefficient of breast tumours.
- Minimum and mean apparent diffusion coefficient perform best and are reproducible.
- 2D regions of interest perform best and provide rapid measurement times.

Keywords Breast cancer · Magnetic resonance imaging · Molecular imaging · Diffusion magnetic resonance imaging · Reproducibility of results and findings

Electronic supplementary material The online version of this article (doi:10.1007/s00330-016-4564-3) contains supplementary material, which is available to authorized users.

✉ Thomas H. Helbich
thomas.helbich@meduniwien.ac.at

¹ Division of Molecular and Gender Imaging, Department of Biomedical Imaging and Image-Guided Therapy, Medical University Vienna, Waehringer Guertel 18-20, 1090 Vienna, Austria

² Department of Biomedical Imaging and Image-Guided Therapy, Medical University Vienna – MR Center of Excellence, Vienna, Austria

³ Department of Pathology, Medical University Vienna, Vienna, Austria

Abbreviations

ADC	Apparent diffusion coefficient
AUC	Area under the curve
CE	Contrast enhanced
CI	Confidence interval
DCIS	Ductal carcinoma in situ
DWI	Diffusion weighted imaging
EPI	Echo planar imaging
ICC	Intra-class correlation
IDC	Invasive ductal carcinoma
ILC	Invasive lobular carcinoma

IPC	Intraductal papillary carcinoma
MPR	Multiplanar reconstruction
MRI	Magnetic resonance imaging
ROC	Receiver operating characteristics
ROI	Region of interest

Introduction

Recently, diffusion-weighted imaging (DWI) has been an increasingly investigated magnetic resonance imaging (MRI) technique for the evaluation of breast lesions [1–3]. DWI measures the random movement of water molecules (i.e. Brownian movement). DWI depicts the diffusivity of the examined tissues, providing a surrogate marker for tissue microstructure and cell density [4]. This diffusivity can be quantified by calculating the apparent diffusion coefficient (ADC). Low ADC values indicate a diffusion restriction, i.e. caused by high cellular density, as can be seen in many malignant breast tumours [5].

In addition to the application of DWI for the differentiation of invasive and non-invasive breast cancers [2] or for the identification of viable lesion parts for ¹H-MR spectroscopy [6], several studies have shown the ability of ADC to differentiate between benign and malignant breast lesions [7, 8]. A recent meta-analysis has shown a wide range of results, with sensitivities ranging from 52 to 100 % and specificities from 33 to 100 % [9].

The reasons for this wide range are most likely attributable to different hardware (field strength, gradients) [10, 11], examination parameters (e.g. different b-values) [12], the DWI field of view [13] or even different post-processing systems [14].

ADC is usually measured by placing regions-of-interest (ROIs) inside the breast lesion. To date, no consensus about how to choose these ROIs exists, although studies on DWI in colorectal cancer have shown that ROI-placement significantly influences ADC-values [15].

Different ROI-placement approaches have been described for DWI in breast imaging: 2D-ROIs covering the part of the lesion displaying the lowest ADC-values [3, 16]; 2D-ROIs covering the whole lesion in one slice [17]; or 3D-ROIs covering the whole lesion [4, 18].

Before the body of evidence on quantitative DWI of the breast can be used to provide general diagnostic thresholds for clinical practice, it is mandatory to obtain data about measurement-dependent ADC disparities.

Furthermore, different authors have investigated either minimum ADC (ADC_{min}) [19, 20] or mean ADC (ADC_{mean}) [21, 22], which will most probably lead to different measured ADC-values and may also influence diagnostic performance.

Thus, the aim of this study was to:

- Investigate whether different ROI-placement approaches influence ADC-values;
- Compare the diagnostic performance and clinical feasibility of these approaches to differentiate benign from malignant breast lesions using ADC_{min}, ADC_{mean}, and maximum ADC (ADC_{max});
- Investigate the measurement times and the inter- and intra-reader reproducibility for these measurement approaches.

Materials and methods

The institutional review board of the Medical University Vienna approved our study. Written, informed consent was obtained from all patients.

Patients

Between September 2007 and December 2011, 626 patients with suspicious findings on mammography or ultrasound, i.e. asymmetric density, architectural distortion, breast mass or microcalcifications (BI-RADS 0, further imaging warranted; BI-RADS 4, suspicious abnormality; BI-RADS 5, highly suggestive for malignancy) underwent breast MRI at our institution. Of these, 150 consecutive patients who fulfilled the following inclusion criteria were retrospectively evaluated: breast lesion visible on MRI; lesion size ≥ 5 mm; histopathological proof of the assessed lesion; and no diagnostic or therapeutic intervention prior to the MRI examination. Of these, three patients were excluded due to technical failure of DWI, resulting in a study population of 147 patients with 149 breast lesions (mean age: 53.2 years, SD 13.4, range 24–86).

Imaging

All patients underwent 3 T-MRI (Tim Trio, Siemens, Erlangen, Germany) in the prone position, using a four-channel breast coil (InVivo, Orlando, FL, USA). In premenopausal women, MRI was performed in the second week of the menstrual cycle [23].

A standardized MRI examination was applied, including a T2w-sequence, a pre-contrast diffusion-weighted sequence and a dynamic contrast-enhanced (CE) (0.1 mmol/kg body weight Gd-DOTA, Dotarem®, Guerbet, France) T1w-sequence [4].

For DWI, an axial, three-acquisition-direction, trace diffusion-weighted, double-refocused, single-shot echo-planar imaging (EPI) sequence with inversion recovery and fat-

suppression was used (TR/TE/TI 13700/83/220 ms; FOV 340x117 mm; 40 slices at 3.5 mm; matrix 192x64 [50 % oversampling]; two averages; b-values 50 and 850 s/mm²; bandwidth 1446 Hz/pixel; 3:19 min) [12].

Monoexponential ADC-maps were automatically calculated by the MR imaging system software from the DWI-images at the two b-values, b₁ and b₂, using the formula $= \frac{\ln(\frac{S_2}{S_1})}{b_1 - b_2}$ with S the signal intensity at the given b-value.

Data analysis

Three radiologists independently performed all ROI-placements:

- Reader 1 (R1): 4 years of experience in breast MRI.
- Reader 2 (R2): 2 years of experience in breast MRI.
- Reader 3 (R3): 3 months of experience in breast MRI.

All were blinded to the histopathological results. R1 repeated the measurements three months after the initial reading.

A second person recorded the measurement time for each reader. Time recording was started when the reader had definitely identified the lesion of interest.

High b-value DWI images were visually assessed for hyperintensities corresponding to enhancing lesions on CE-MRI. Lesion size was determined on the CE-MRI images and was defined as the largest diameter of the lesion. OSIRIX (Pixmeo SARL, Bernex, CH) [24], was used for the assessment of the ADC-maps.

Three different ROI-placement approaches were applied by each reader (Figs. 1, 2 and 3).

- One manually drawn 2D-ROI, covering the area, visually assessed, with the lowest ADC-values inside the lesion (small 2D-ROI).

- One 2D-ROI, covering the whole lesion on the slice, visually assessed, with the lowest ADC-values (large 2D-ROI).
- Multiple, manually drawn large 2D-ROIs on each slice containing the lesion of interest, which were then combined to create a 3D-ROI using the OSIRIX ROI-volume-tool.

Partial volume effects due to surrounding tissue and necrosis, as identified from the T2w- and CE-MRI, were avoided as far as possible by sparing the lesion borders (Figs. 1, 2 and 3) and drawing the ROIs around obvious necrosis. Clip artifacts were not an issue, as all MRI examinations were performed before any biopsy.

ADC_{min}, ADC_{mean}, ADC_{max} and ROI sizes were determined. The reference standard was histopathology in all cases. Histopathology specimens were obtained either by image-guided biopsy or open surgery. Histopathological analysis was performed by two board-certified pathologists who specialized in breast pathology. Diagnostic procedures were performed according to the European guidelines for quality assurance in breast cancer screening and diagnosis [25].

Statistical analysis

Statistical analysis was performed using SPSS 19.0 (IBM Corp., Armonk, NY, USA), MedCalc 12 (MedCalc Software, Ostend, Belgium), and the online receiver operating characteristics (ROC) software StAR [26]. All calculations were performed on a per-lesion basis. Nominal data, such as lesion type, are presented using absolute frequencies and percentages. Differences in ROI-sizes between readers were calculated using a paired samples t-test. Differences in ADC and diagnostic performance between the different measurement approaches were calculated from the averaged results of all three readers (one result

Fig. 1 Schematic representation of the different ROI-placement approaches. Image (a) shows a breast lesion with heterogeneous ADC-values. The different ROI (white lines) placement approaches were: a small-2D ROI covering the part of the lesion with the lowest ADC-values (b); a large 2D-ROI covering the whole lesion on one slice (c); and a 3D-ROI covering the whole lesion on all slices (d). ADC apparent diffusion coefficient, ROI region of interest

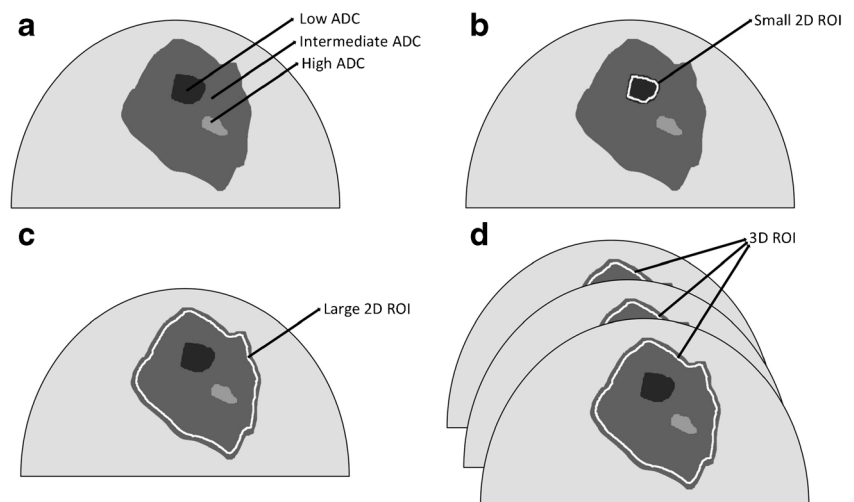
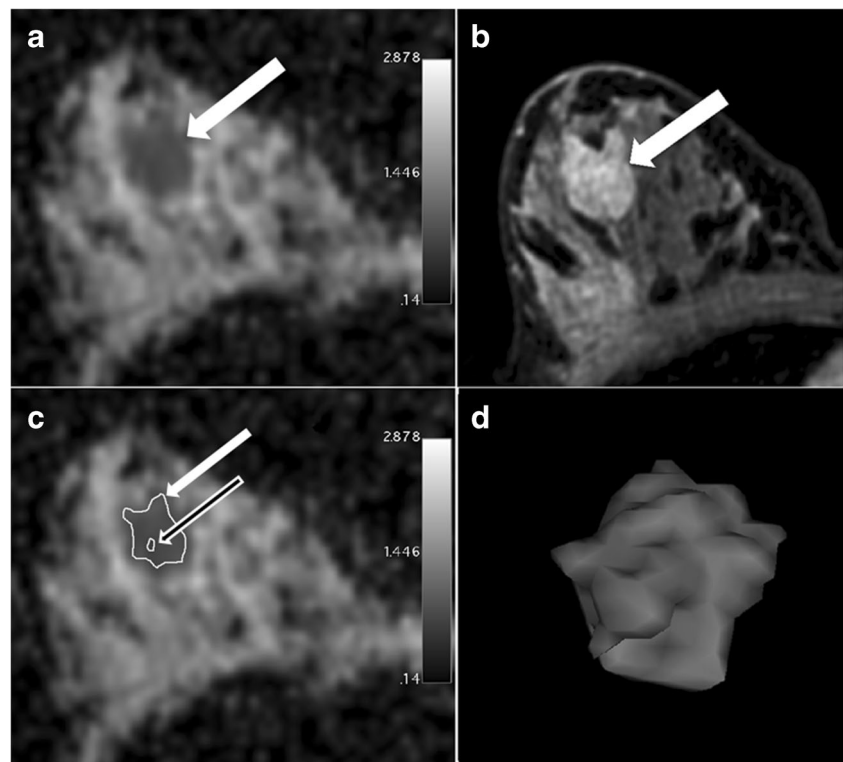


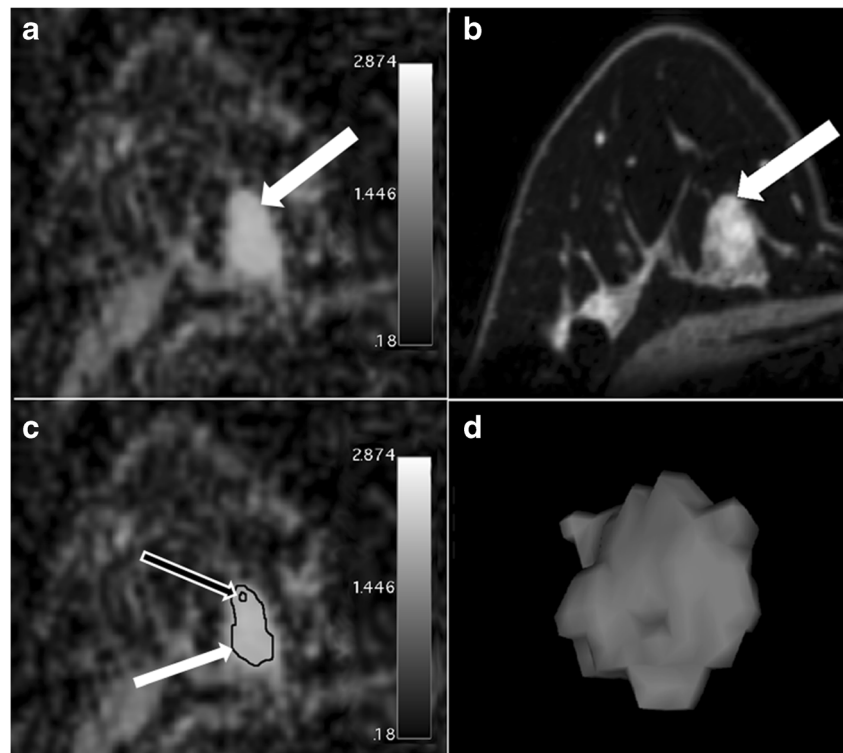
Fig. 2 Grade 3 invasive ductal cancer (thick white arrows) verified by histopathology in the right breast of a 39-year-old woman. Axial ADC-map (a) and corresponding axial contrast-enhanced T1 image (b). Image (c) shows the small 2D-ROI (black/white arrow), as well as the ROI covering the whole lesion in this slice (thin white arrow) on the ADC-map. Three-dimensional rendering of the whole lesion volume covered by the 3D-ROI (d). ADC apparent diffusion coefficient, ROI region of interest



per reader). After testing for normal distribution using the Kolmogorov-Smirnov test for independent variables and the McNemar test for paired sample variables, metric data like ADC are presented using median and interquartile ranges. Differences in average ADC-values for different

groups and subgroups (e.g. stratified by size) were calculated using the Mann-Whitney U and Wilcoxon's matched pairs test. ROC-analysis was performed to compare diagnostic performance between the readers, ROI-types, ADC-parameters and between mass and non-mass lesions.

Fig. 3 Fibroadenoma (thick white arrows) verified by histopathology in the right breast of a 45-year-old woman. Axial ADC-map (a) and corresponding axial contrast-enhanced T1 image (b). Image (c) shows the small 2D-ROI (black/white arrow), as well as the ROI covering the whole lesion in this slice (thin white arrow) on the ADC map. Three-dimensional rendering of the whole lesion volume covered by the 3D-ROI (d). ADC apparent diffusion coefficient, ROI region of interest



Pearson’s correlation coefficient was used to correlate measurement time and lesion size. Intra-class correlation (ICC) was used to determine inter- and intra-reader agreement. A p -value ≤ 0.05 was considered a significant result.

Results

Detailed histopathological results are displayed in Table 1.

There were 29 (19.5 %) non-mass and 120 (80.5 %) mass lesions according to CE-MRI. Median lesion size was 23 mm (range: 5–106 mm). Malignant lesions (5–106 mm, median 26.0 mm) were significantly larger ($p < .001$) than benign lesions (5–60 mm, median 14.5 mm). Non-mass lesions (median size 31 mm) were significantly larger ($p = .009$) than mass lesions (22 mm).

Comparison of ADC-values of the different ROI-placement approaches

The results for the comparison of the different approaches are displayed in Fig. 4.

ADC-values of benign and malignant lesions were significantly different for all minimum, mean and maximum values, independent of the ROI-placement approach ($p < .001$), except for the ADCmax of the 3D-ROI ($p = .125$).

Table 1 Histopathological results of the patient cohort, by enhancement pattern

		Non-mass (%)	Mass (%)	Total (%)
Benign	Mastitis	0 (0)	1 (100)	1 (.7)
	Fibroadenoma	2 (11.8)	15 (88.2)	17 (11.4)
	Intraductal epithelial proliferation without atypia	1 (33.3)	2 (66.7)	3 (2)
	Papilloma	1 (33.3)	2 (66.7)	3 (2)
	Pseudoangiomatous changes	1 (100)	0 (0)	1 (.7)
	Scar tissue	1 (100)	0 (0)	1 (.7)
	Fibrocystic changes	6 (42.9)	8 (57.1)	14 (9.4)
	Total	12 (30)	28 (70)	40 (26.8)
	Malignant	DCIS	8 (53.3)	7 (46.7)
IDC		7 (8.4)	76 (91.6)	83 (55.7)
ILC		2 (22.2)	7 (77.8)	9 (6)
Mucinous		0 (0)	1 (100)	1 (.7)
IPC		0 (0)	1 (100)	1 (.7)
Total		17 (15.6)	92 (84.4)	109 (73.2)
Total	29 (19.5)	120 (80.5)	149 (100)	

DCIS ductal carcinoma in situ, IDC invasive ductal carcinoma, ILC invasive lobular carcinoma, IPC intraductal papillary carcinoma

ADCmin, ADCmean and ADCmax of benign ($p < .001$ -.003) and malignant ($p < .001$) lesions differed significantly between the three ROI-placement approaches. The only exception was for the ADCmean of the large 2D-ROI versus the 3D-ROI ($p = .346$).

ROC analysis

The results of the ROC analysis are displayed in Table 2, Fig. 5 and Supplemental Table 1. Overall, areas under the receiver operating characteristic curve (AUC) ranged between .583 (ADCmax of the 3D-ROI) and .956 (ADCmin of the large 2D-ROI). Generally, ADCmin performed best, independent of the ROI-placement approach, followed by the ADCmean using 2D-ROIs, while the ADCmean of the 3D-ROIs and ADCmax performed significantly worse.

ADC performed worse in non-mass (AUC .637–.728), than in mass lesions (AUC .959–.97) when using ADCmean, independent of the ROI-placement approach ($0.004 < p < 0.016$), and when using ADCmax obtained from the small 2D-ROIs (AUC 0.642 vs. 0.913, $p = .015$). For the other combinations of ROI-placement approaches and ADC-parameters, AUC did not differ significantly ($.051 < p < .509$) between mass and non-mass lesions (Supplemental Table 2).

When looking at the mass lesions only, ADCmin and ADCmean performed comparably well (AUC .952–.982), independent of the ROI-placement approach ($.063 < p < .098$), with the exception of ADCmin obtained from the large 2D-ROI (AUC .982), which performed significantly better than ADCmin obtained from the 3D-ROI (AUC .952, $p = .022$) (Supplemental Table 3). In the non-mass lesions, ADCmin obtained from the large 2D- and 3D-ROI performed best (AUC .841), but the difference was only significant compared to ADCmean obtained from the 3D-ROIs and ADCmax obtained from the large 2D-ROIs (Supplemental Table 4).

When stratified by size, the AUC difference between the ROI-placement approaches was minimal in lesions ≤ 1 cm ($n = 20$, .881–.940). In the lesions > 1 cm ($n = 129$), AUCs differed between the ROI-placement approaches, with results comparable to those of the whole population (.554–.962).

Measurement time

Median measurement times differed significantly ($p < .001$) between the ROI-placement approaches, with 7 s (range: 3.3–23.7 s) for the small 2D-ROIs, 9.3 s (3.7–31 s) for the large 2D-ROIs, and 34.3 s (3.7–432 s) for the 3D-ROIs. Measurement times correlated significantly with lesion size ($p < .001$).

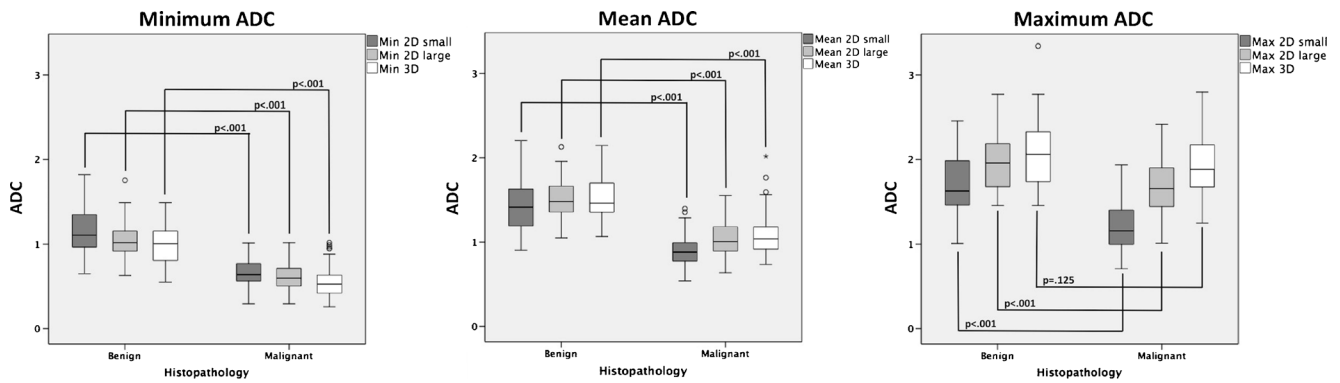


Fig. 4 Boxplots showing the minimum, mean and maximum ADC-values of the different ROI placement approaches. ADC-values for benign and malignant lesions were significantly different for all ROI placement approaches and parameters ($p < .001$), except for maximum

ADC of the 3D-ROI ($p = .125$); ADC values are displayed in $\times 10^{-3} \text{ mm}^2/\text{s}$. ADC apparent diffusion coefficient, ROI region of interest, Min minimum, Max maximum

Inter- and intra-reader reproducibility analysis

The results of the reproducibility analysis are displayed in Table 2.

Inter- and intra-reader agreement was generally high for ADCmin (ICC .737–.861) and ADCmean (.721–.885), and lower for ADCmax (.301–.78).

ROI size

The size of the small 2D-ROIs (range: 1–149 mm^2) showed significant inter- ($p < .001$) and intra-reader ($p = .018$) differences, with R1 generally drawing smaller ROIs (mean 4.9 mm^2 and 4.1 mm^2) than R2 (21.2 mm^2) and R3 (13.8 mm^2).

Concerning the large 2D-ROIs, R1 drew significantly smaller ROIs during his first reading session than R2 ($p = .05$). Otherwise, there was no significant difference in ROI size between the readers ($.054 < p < .32$). In the 3D-

ROIs, there were no significant differences between the readers ($.077 < p < .987$).

Discussion

Our study demonstrates that the results of ADC-value measurements in breast tumours are significantly influenced by ROI-placement. ADCmin and ADCmean acquired from 2D-ROIs perform best for the differentiation of benign and malignant breast lesions, and are highly reproducible, with rapid measurement. 3D-ROIs and ADCmax perform significantly worse.

The results of this study show that the acquired ADC of benign and malignant breast lesions is highly dependent on ROI-placement. This reflects the internal structural heterogeneity of breast lesions, which leads to substantial differences in measured ADC-values, depending on whether only small lesion areas with relatively homogeneous ADC, larger lesion

Table 2 Areas under the ROC curve and inter- and intra-reader ICCs for the different measurement approaches

	AUC	CI	ICC*	CI*	ICC**	CI**
Minimum 2D large	0.956	0.923 - 0.989	0.7366	0.6719 - 0.7932	0.8538	0.8035 - 0.8920
Minimum 2D small	0.948	0.908 - 0.988	0.7957	0.7411 - 0.8419	0.8452	0.7922 - 0.8855
Mean 2D small	0.940	0.902 - 0.979	0.7623	0.6344 - 0.8415	0.8822	0.8408 - 0.9134
Minimum 3D	0.928	0.885 - 0.971	0.7448	0.6790 - 0.8012	0.8607	0.8125 - 0.8972
Mean 2D large	0.925	0.882 - 0.967	0.8486	0.8030 - 0.8853	0.8848	0.8416 - 0.9164
Mean 3D	0.906	0.859 - 0.953	0.7208	0.6531 - 0.7803	0.8820	0.8405 - 0.9132
Maximum 2D small	0.870	0.804 - 0.936	0.4750	0.2812 - 0.6220	0.7795	0.7048 - 0.8366
Maximum 2D large	0.717	0.629 - 0.804	0.3011	0.02149 - 0.5370	0.6725	0.5464 - 0.7638
Maximum 3D	0.582	0.482 - 0.682	0.5498	0.4033 - 0.6650	0.7483	0.6631 - 0.8135

* inter-reader

** intra-reader

ROC receiver operating characteristics, AUC area under the curve, CI confidence interval, ICC intra-class correlation

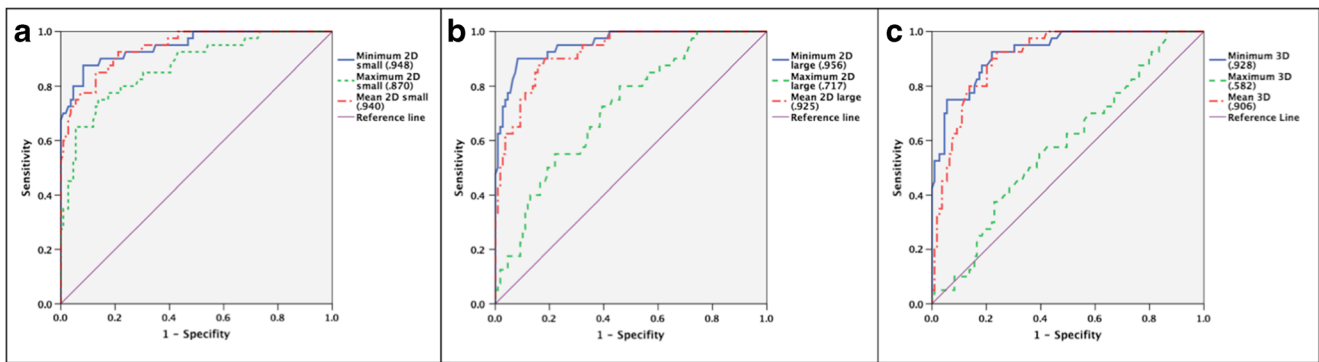


Fig. 5 ROC curves and AUC (in brackets) for the minimum, mean and maximum ADC of the different ROI placement approaches – small 2D-ROI (a), large 2D-ROI (b) and 3D-ROI (c). In general, minimum and mean ADC of the 2D-ROIs performed best, while maximum ADC

performed worst. *Min* minimum, *Max* maximum, *ROC* receiver operating characteristics, *ROI* region of interest, *AUC* area under the curve, *ADC* apparent diffusion coefficient

areas, or even the whole lesion are included in the ROI. A similar effect has been described in rectal cancer [15]. Recently, it has been reported that ADC-values of breast lesions were significantly different between small and large 2D-ROIs, with the small ROIs generally performing better than large ones [27–29]. Thus, the ROI-placement approach seems to have an influence on the diagnostic performance of DWI for the breast and other tumours.

Furthermore, the selection of ADC_{min}, ADC_{mean} or ADC_{max} has a substantial influence on diagnostic performance. Our study shows that ADC_{min} and ADC_{mean} obtained from 2D-ROIs are the most accurate parameters for the differentiation of benign and malignant breast lesions.

Considering low ADC-values as diagnostic for breast cancer, it may be assumed that ADC_{min} represents the most malignant part of the tumour. Our study design was not able to demonstrate what causes minimum ADC-values through direct histopathological correlation. However, Guo et al. have shown that there is a general inverse correlation between the ADC and the cellular density of breast lesions [30].

Even though the tumour part with the lowest ADC is always covered when using a 3D-ROI, in our study, ADC_{min} obtained from the small, as well as the large 2D-ROI, performed better. This could be attributed to one potential pitfall of ADC_{min}: it is susceptible to partial volume effects. The risk of inadvertently measuring areas of suppressed fat is higher in large ROIs that cover multiple slices. Therefore, the borders of the ROI need to be placed carefully when using this approach.

While ADC_{min} represents only the most relevant part of the tumour, ADC_{mean} also includes the information from voxels that contain less malignant or even necrotic tumour parts. Based on our results, this effect is negligible in the 2D-ROIs, but becomes more problematic in 3D-ROIs. However, this averaging effect makes ADC_{mean} less susceptible to partial volume effects.

ADC_{max} is a parameter that has rarely been investigated. In our study, ADC_{max} performed significantly worse than

ADC_{min} and ADC_{mean}, independent of the ROI-placement approach, which is in accordance with a recent study by Hirano et al. [20]. This again can be attributed to the structural heterogeneity of many breast lesions, leading to the inclusion of less malignant or even necrotic lesion parts, and thus, altering the results of the measured ADC_{max}.

Therefore, ADC_{min} and ADC_{mean} are reliable parameters for the differentiation of benign and malignant breast lesions, while ADC_{max} should not be considered.

Problematic entities in breast imaging are non-mass lesions. Previous studies have shown that ADC performs worse for the differentiation of benign and malignant breast lesions in non-mass lesions than in mass lesions [31, 32], even though Iima et al. [33] have shown that ADC has the potential to differentiate high-grade from low-grade DCIS.

ADC also performed worse in non-mass than in mass lesions in our study; however, this difference was only significant when using ADC_{mean} (independent of ROI placement approach) and ADC_{max} obtained from the small 2D-ROIs. The inferiority of ADC_{mean} in non-mass lesions is probably due to partial volume effects: nearly half the malignant non-mass lesions in our study were DCIS, which frequently presents as a non-mass lesion. This tumour type stems from the ductal epithelium of the breast and consists of neoplastic cells, but does not infiltrate through the basal membrane. Thus, the tissue between ducts is less affected by tumour growth, leading to an increased ADC_{mean}, while ADC_{min} remains low.

Based on our results, it was not possible to find an optimal combination of ROI-placement approach and ADC-parameter for the differentiation of benign and malignant non-mass lesions. While ADC_{min} obtained from the large 2D- and the 3D-ROI performed best, their performance was not significantly better than most of the other possible combinations. This can possibly be attributed to the relatively low number of non-mass lesions ($n = 29$) in our patient collective.

One crucial factor for the usefulness of a quantitative imaging method is its reproducibility [34]. In our study,

ADC_{min} and ADC_{mean} generally showed high inter- and intra-reader agreement, independent of the ROI-placement approach. This is in agreement with other studies, which reported that the reproducibility of ADC measurements is high. Bogner et al. [35] showed good inter-reader agreement when using small 2D-ROIs and ADC_{mean}. Dijkstra et al. [36] found no significant difference between the ADC-values of breast lesions, as assessed by three different readers, using whole tumour ROIs. However, the authors did not report whether the whole lesion was measured two- or three-dimensionally. Two-dimensional ROIs covering the whole lesion on one slice have been reported to provide the best reproducibility when measuring the ADC_{mean} of breast lesions [27, 37], which is in agreement with our results. To our knowledge, only Nogueira et al. have reported better inter-reader agreement for small 2D-ROIs [28]. However, none of these studies have reported significance levels for the differences in reproducibility.

In rectal cancer, Lambregts et al. [15] reported the best reproducibility when using 3D-ROIs that covered the whole lesion (ICC .91), compared to large- (ICC .53) and small 2D-ROIs (ICC .63). This can probably be attributed to the different tumour morphology of rectal cancer compared to breast lesions. While rectal cancer often is a rather clearly demarcated tumour growing into the lumen of the rectum, breast lesions may present as mass or non-mass lesions, the latter being much harder to exactly demarcate. Furthermore, in that study, the small 2D-ROI was not placed in the region with the lowest ADC, but in the most solid tumour part based on the T2w-images. In our study, agreement was only weak-to-moderate when measuring ADC_{max}, further limiting the usefulness of this parameter.

Measurement time is another important factor that limits the applicability of an imaging method. In our study, median measurement times were lowest for the placement of the small 2D-ROIs. Placement of the large 2D-ROIs took significantly longer; however, in absolute values, the difference was only 2 s, which can probably be considered negligible. Placement of the 3D-ROIs often took up to several minutes, especially when dealing with large, heterogeneous tumours, substantially reducing the feasibility of 3D-ROIs in a clinical setting. Measurement times correlated significantly with tumour size for all ROI-placement approaches: in large tumours, it took the readers time to identify the region with the lowest ADC-values to place the small ROI, and it was often necessary to draw complex ROIs around necrotic lesion parts to place the large 2D-ROI and 3D-ROI. Thus, measurement time also contributes to the fact that 2D-ROIs are more usable than 3D-ROIs.

In the small 2D-ROIs, ROI sizes showed significant inter- and intra-reader differences. The readers were not given any specifications about minimum or maximum ROI size and the ROI was to be placed to cover the region with the lowest ADC

identified by visual assessment. Especially in large, heterogeneous tumours, it is quite probable that the readers did not always identify the same region as the one with the lowest ADC, thus leading to differently sized small 2D-ROIs. Furthermore, the readers were free to adjust the windowing levels to their convenience, which may have influenced the readers' perception of the extent of the region with the lowest ADC. Finally, since lesion borders were to be avoided to minimize partial volume effects, different extents of this "safety margin" may have altered ROI size.

In the large 2D-ROIs, ROI size was significantly different only between one pair of readers. This can also be attributed to the effects mentioned above, since this ROI was placed on the slice with the lowest overall ADC, again identified by visual assessment. No significant differences were found between the readers in the 3D-ROIs, since no visual identification of a specific tumour part was necessary and the often-large extent of the ROI reduced the effect of the aforementioned safety margins.

We performed DWI using two b-values (50 and 850 s/mm²). Despite some discussion about whether the use of more b-values could better represent the signal decline in DWI with increasing b-values, and lead to more accurate ADC-values, it has been shown [12, 38], that this does not alter the capability of ADC to differentiate between benign and malignant breast lesions. A recent meta-analysis by Dorrius et al. [9] has, however, shown that in 1.5 T, the used b-values significantly influence the measured ADC, which is another factor that has to be taken into account when trying to compare quantitative results in breast DWI.

One limitation of this study is its retrospective nature. This implies that the actual ADC measurements were not used in clinical decision-making. Consequently, our study does not provide any data about whether patient management would be altered by different ROI-measurement approaches. In addition, a spatial correlation of areas with specific (e.g. low or minimum) ADC-values and histopathological findings, such as cellularity, fibrosis or vascularization, could not be performed. This, however, is difficult to realize in clinical practice, as there is, as yet, no accurate DWI-guided core needle biopsy designed to subsample specific regions in suspicious breast lesions. Rather, MRI-only lesions are biopsied using 9-G vacuum-assisted biopsy, which is targeted based on contrast-enhanced images [23], as most DWI sequences show some amount of spatial distortion [35, 39]. A systematic approach in the defined group of patients, as employed in this study, allowed us to investigate and compare different ROI measurements and identify those most promising for clinical application. A prospective approach would therefore not have led to different results given the rationale and methods of this study.

Another limitation is that we did not evaluate the performance of non-manually drawn, geometric ROIs, as has been

performed in some previous studies [16, 40, 41]. While these ROIs might have an advantage with regard to the speed of ROI placement, it would seem that placing a strictly geometric ROI in an irregularly shaped lesion would increase the pitfall of partial volume effects, thus leading to altered measurement results.

Furthermore, our patient collective contains a high relative number of malignant lesions compared to benign lesions. This is due to the fact that our institution is a major breast care centre and many patients are referred either because of symptomatic breast tumours or for second-look examinations after imaging abnormalities were detected in other institutions. Thus, our study population was not recruited from a screening population, leading to an increased fraction of malignant lesions.

In conclusion, the results of ADC-value measurements in breast tumours are significantly influenced by ROI placement. ADC_{min} and ADC_{mean} acquired from 2D-ROIs performed best for the differentiation of benign and malignant breast lesions, and are highly reproducible, with rapid measurement. 3D-ROIs and ADC_{max} perform significantly worse.

Acknowledgments The scientific guarantor of this publication is Thomas Helbich. The authors of this manuscript declare no relationships with any companies whose products or services may be related to the subject matter of the article. This study has received funding by projects no. 13652 funded by Austrian National Bank 'Jubilaumsfond' and no. 10029 funded by the Medical-Scientific Funds of the Mayor of Vienna.

One of the authors (Pascal Baltzer) has significant statistical expertise. Institutional Review Board approval was obtained. Written informed consent was obtained from all subjects (patients) in this study. Approval from the institutional animal care committee was not required because no animals were involved in this study. Some study subjects or cohorts have been previously reported in:

Pinker K, Bickel H, Helbich TH, et al. Combined contrast-enhanced magnetic resonance and diffusion-weighted imaging reading adapted to the "Breast Imaging Reporting and Data System" for multiparametric 3-T imaging of breast lesions. *Eur Radiol*. 2013;23(7):1791–802. (*n* = 85)

Pinker K, Bogner W, Baltzer P, et al. Improved diagnostic accuracy with multiparametric magnetic resonance imaging of the breast using dynamic contrast-enhanced magnetic resonance imaging, diffusion-weighted imaging and 3-dimensional proton magnetic resonance spectroscopic imaging. *Investigative radiology*. 2014;49(6):421–30. (*n* = 52)

Pinker K, Bogner W, Baltzer P, et al. Improved differentiation of benign and malignant breast tumours with multiparametric 18fluorodeoxyglucose positron emission tomography magnetic resonance imaging: a feasibility study. *Clinical cancer research : an official journal of the American Association for Cancer Research*. 2014;20(13):3540–9. (*n* = 39)

Bickel H, Pinker-Domenig K, Bogner W, et al. Quantitative apparent diffusion coefficient as a noninvasive imaging biomarker for the differentiation of invasive breast cancer and ductal carcinoma in situ. *Investigative radiology*. 2015;50(2):95–100. (*n* = 83)

Methodology: retrospective, diagnostic or prognostic study, performed at one institution.

References

- Bogner W, Pinker K, Zaric O et al (2015) Bilateral diffusion-weighted MR imaging of breast tumors with submillimeter resolution using readout-segmented echo-planar imaging at 7 T. *Radiology* 274:74–84
- Bickel H, Pinker-Domenig K, Bogner W et al (2015) Quantitative apparent diffusion coefficient as a noninvasive imaging biomarker for the differentiation of invasive breast cancer and ductal carcinoma in situ. *Invest Radiol* 50:95–100
- Woodhams R, Matsunaga K, Kan S et al (2005) ADC mapping of benign and malignant breast tumors. *Magn Reson Med Sci* 4:35–42
- Pinker K, Bickel H, Helbich TH et al (2013) Combined contrast-enhanced magnetic resonance and diffusion-weighted imaging reading adapted to the "Breast Imaging Reporting and Data System" for multiparametric 3-T imaging of breast lesions. *Eur Radiol* 23:1791–1802
- Spick C, Pinker-Domenig K, Rudas M, Helbich TH, Baltzer PA (2014) MRI-only lesions: application of diffusion-weighted imaging obviates unnecessary MR-guided breast biopsies. *Eur Radiol* 24:1204–1210
- Sun K, Chai W, Fu C et al (2015) Diffusion-weighted imaging-guided MR spectroscopy in breast lesions using readout-segmented echo-planar imaging. *Eur Radiol*. doi:10.1007/s00330-015-4000-0
- Woodhams R, Matsunaga K, Iwabuchi K et al (2005) Diffusion-weighted imaging of malignant breast tumors: the usefulness of apparent diffusion coefficient (ADC) value and ADC map for the detection of malignant breast tumors and evaluation of cancer extension. *J Comput Assist Tomogr* 29:644–649
- Baltzer PA, Schafer A, Dietzel M et al (2011) Diffusion tensor magnetic resonance imaging of the breast: a pilot study. *Eur Radiol* 21:1–10
- Dorrius MD, Dijkstra H, Oudkerk M, Sijens PE (2014) Effect of b value and pre-admission of contrast on diagnostic accuracy of 1.5-T breast DWI: a systematic review and meta-analysis. *Eur Radiol* 24: 2835–2847
- Lourenco AP, Donegan L, Khalil H, Mainiero MB (2014) Improving outcomes of screening breast MRI with practice evolution: initial clinical experience with 3T compared to 1.5T. *J Magn Reson Imaging* 39:535–539
- Gruber S, Minarikova L, Pinker K et al (2016) Diffusion-weighted imaging of breast tumours at 3 Tesla and 7 Tesla: a comparison. *Eur Radiol* 26:1466–1473
- Bogner W, Gruber S, Pinker K et al (2009) Diffusion-weighted MR for differentiation of breast lesions at 3.0 T: how does selection of diffusion protocols affect diagnosis? *Radiology* 253:341–351
- Barentsz MW, Taviani V, Chang JM et al (2015) Assessment of tumor morphology on diffusion-weighted (DWI) breast MRI: diagnostic value of reduced field of view DWI. *J Magn Reson Imaging* 42:1656–1665
- Clauser P, Marcon M, Maieron M, Zuiani C, Bazzocchi M, Baltzer PA (2015) Is there a systematic bias of apparent diffusion coefficient (ADC) measurements of the breast if measured on different workstations? an inter- and intra-reader agreement study. *Eur Radiol*. doi:10.1007/s00330-015-4051-2
- Lambregts DM, Beets GL, Maas M et al (2011) Tumour ADC measurements in rectal cancer: effect of ROI methods on ADC values and interobserver variability. *Eur Radiol* 21:2567–2574
- Hatakenaka M, Soeda H, Yabuuchi H et al (2008) Apparent diffusion coefficients of breast tumors: clinical application. *Magn Reson Med Sci* 7:23–29
- Choi SY, Chang YW, Park HJ, Kim HJ, Hong SS, Seo DY (2012) Correlation of the apparent diffusion coefficient values on

- diffusion-weighted imaging with prognostic factors for breast cancer. *Br J Radiol* 85:474–479
18. Iaconi C, Giannelli M, Marini C et al (2010) The role of mean diffusivity (MD) as a predictive index of the response to chemotherapy in locally advanced breast cancer: a preliminary study. *Eur Radiol* 20:303–308
 19. Mori N, Ota H, Mugikura S et al (2013) Detection of invasive components in cases of breast ductal carcinoma in situ on biopsy by using apparent diffusion coefficient MR parameters. *Eur Radiol* 23:2705–2712
 20. Hirano M, Satake H, Ishigaki S, Ikeda M, Kawai H, Naganawa S (2012) Diffusion-weighted imaging of breast masses: comparison of diagnostic performance using various apparent diffusion coefficient parameters. *AJR Am J Roentgenol* 198:717–722
 21. Partridge SC, Rahbar H, Murthy R et al (2011) Improved diagnostic accuracy of breast MRI through combined apparent diffusion coefficients and dynamic contrast-enhanced kinetics. *Magn Reson Med* 65:1759–1767
 22. Pinker K, Bogner W, Baltzer P et al (2014) Improved diagnostic accuracy with multiparametric magnetic resonance imaging of the breast using dynamic contrast-enhanced magnetic resonance imaging, diffusion-weighted imaging, and 3-dimensional proton magnetic resonance spectroscopic imaging. *Invest Radiol* 49:421–430
 23. Sardanelli F, Boetes C, Borisch B et al (2010) Magnetic resonance imaging of the breast: recommendations from the EUSOMA working group. *Eur J Cancer* 46:1296–1316
 24. Rosset A, Spadola L, Pysker L, Ratib O (2006) Informatics in radiology (infoRAD): navigating the fifth dimension: innovative interface for multidimensional multimodality image navigation. *Radiographics* 26:299–308
 25. Perry N, Broeders M, de Wolf C, Tomberg S, Holland R, von Karsa L (2008) European guidelines for quality assurance in breast cancer screening and diagnosis. Fourth edition—summary document. *Ann Oncol* 19:614–622
 26. Vergara IA, Norambuena T, Ferrada E, Slater AW, Melo F (2008) StAR: a simple tool for the statistical comparison of ROC curves. *BMC Bioinform* 9:265
 27. Arponent O, Sudah M, Masarwah A (2015) Diffusion-weighted imaging in 3.0 Tesla breast MRI: diagnostic performance and tumor characterization using small subregions vs. whole tumor regions of interest. *PLoS One* 10:e0138702
 28. Nogueira L, Brandao S, Matos E et al (2015) Region of interest demarcation for quantification of the apparent diffusion coefficient in breast lesions and its interobserver variability. *Diagn Interv Radiol* 21:123–127
 29. Min Q, Shao K, Zhai L et al (2015) Differential diagnosis of benign and malignant breast masses using diffusion-weighted magnetic resonance imaging. *World J Surg Oncol* 13:32
 30. Guo Y, Cai YQ, Cai ZL et al (2002) Differentiation of clinically benign and malignant breast lesions using diffusion-weighted imaging. *J Magn Reson Imaging* 16:172–178
 31. Kul S, Eyuboglu I, Cansu A, Alhan E (2014) Diagnostic efficacy of the diffusion weighted imaging in the characterization of different types of breast lesions. *J Magn Reson Imaging* 40:1158–1164
 32. Partridge SC, Mullins CD, Kurland BF et al (2010) Apparent diffusion coefficient values for discriminating benign and malignant breast MRI lesions: effects of lesion type and size. *AJR Am J Roentgenol* 194:1664–1673
 33. Iima M, Le Bihan D, Okumura R et al (2011) Apparent diffusion coefficient as an MR imaging biomarker of low-risk ductal carcinoma in situ: a pilot study. *Radiology* 260:364–372
 34. (2010) European Society of Radiology. white paper on imaging biomarkers. *Insights Imag* 1:42–45
 35. Bogner W, Pinker-Domenig K, Bickel H et al (2012) Readout-segmented echo-planar imaging improves the diagnostic performance of diffusion-weighted MR breast examinations at 3.0 T. *Radiology* 263:64–76
 36. Dijkstra H, Dorrius MD, Wielema M et al (2016) Semi-automated quantitative intravoxel incoherent motion analysis and its implementation in breast diffusion-weighted imaging. *J Magn Reson Imaging* 43:1122–1131
 37. Giannotti E, Waugh S, Priba L, Davis Z, Crowe E, Vinnicombe S (2015) Assessment and quantification of sources of variability in breast apparent diffusion coefficient (ADC) measurements at diffusion weighted imaging. *Eur J Radiol* 84:1729–1736
 38. Pereira FP, Martins G, Figueiredo E et al (2009) Assessment of breast lesions with diffusion-weighted MRI: comparing the use of different b values. *AJR Am J Roentgenol* 193:1030–1035
 39. Baltzer PAT, Renz DM, Herrmann KH et al (2009) Diffusion-weighted imaging (DWI) in MR mammography (MRM): clinical comparison of echo planar imaging (EPI) and half-Fourier single-shot turbo spin echo (HASTE) diffusion techniques. *Eur Radiol* 19:1612–1620
 40. Lo GG, Ai V, Chan JK et al (2009) Diffusion-weighted magnetic resonance imaging of breast lesions: first experiences at 3 T. *J Comput Assist Tomogr* 33:63–69
 41. Kamitani T, Matsuo Y, Yabuuchi H et al (2013) Correlations between apparent diffusion coefficient values and prognostic factors of breast cancer. *Magn Reson Med Sci* 12:193–199